



HAL
open science

Modulation Instability in a dispersion oscillating fiber pumped by a broad band pulse

C Fourcade-Dutin, D Bigourd

► **To cite this version:**

C Fourcade-Dutin, D Bigourd. Modulation Instability in a dispersion oscillating fiber pumped by a broad band pulse. *Journal of Modern Optics*, 2017, 64 (5), pp.500-506. 10.1080/09500340.2016.1244295 . hal-03149339

HAL Id: hal-03149339

<https://hal.science/hal-03149339>

Submitted on 22 Feb 2021

HAL is a multi-disciplinary open access archive for the deposit and dissemination of scientific research documents, whether they are published or not. The documents may come from teaching and research institutions in France or abroad, or from public or private research centers.

L'archive ouverte pluridisciplinaire **HAL**, est destinée au dépôt et à la diffusion de documents scientifiques de niveau recherche, publiés ou non, émanant des établissements d'enseignement et de recherche français ou étrangers, des laboratoires publics ou privés.

To appear in the *Journal of Modern Optics*
 Vol. 00, No. 00, 00 Month 20XX, 1–10

Modulation Instability in a dispersion oscillating fiber pumped by a broad band pulse

C. Fourcade-Dutin and D. Bigourd^{a*}

^a*Institut FEMTO-ST, Département d'Optique, UMR 6174, Université Bourgogne Franche-Comté-CNRS,
 25030 Besançon, France*

(Mai 2016)

We numerically investigate the modulation instability generated in a dispersion oscillating fiber pumped by a chirped pulse with a broad bandwidth. We highlight that the side bands are wide, not symmetric in frequency about the pump and several instantaneous side bands can spectrally overlap with each other in one side while they are well located in the other side. We also show that the spectral distribution can be intuitively explained with an analogy in which the fiber is pumped by a tuneable continuous wave.

Keywords: Modulation instability, parametric amplification, dispersive oscillating fiber.

1. Introduction

Modulation instability (MI) has been widely investigated in optical fibers and is often interpreted in the spectral domain as a four wave mixing (FWM) process or optical parametric amplification [1, 2]. This process is originated from a weak perturbation of a steady state in a medium with an equilibrium between dispersion and nonlinear effects. When an intense continuous wave (CW) or quasi-CW propagates in a fiber, side bands can grow from noise if all the involved waves are phase matched. The spectral features of the generated bands depend on the nonlinear coefficient and the dispersion profile of the fiber. The spectrum is usually symmetric in frequency about the pump due to the linear phase matching factor that depends only on the even order dispersion terms though asymmetry can arise from the stimulated Raman scattering [2] or from the high-order FWM in a saturated regime [3]. The emergence of these side bands has been demonstrated in various configurations in fibers with anomalous [4] and normal dispersion regimes with negative high order terms [5], or in birefringence fiber [6]... More complex dispersion properties have also been designed to tailor the spectral bands. For example, MI has been generated when a CW pumps a dispersion oscillating fiber (DOF) in which the dispersion evolves periodically along the fiber. In this case, multiple discrete side bands are generated in the THz range due to a quasi-phase matching condition [7–10] but the bandwidth is relatively narrow. Recently, other complex longitudinal evolutions of the dispersion have been employed to engineer the band properties, for example to broaden the spectral width of the side bands [11, 12]. In this manuscript, we prefer to vary the pumping scheme instead of designing a fiber with a specific dispersion landscape. We consider a DOF with a single period pumped by a chirped pump pulse with large bandwidth to enhance the spectral broadening of the bands.

Parametric amplification has been recently investigated in a homogeneous fiber pumped by a chirped pulse with a broad bandwidth [13, 14] and the broad band pulse allows the amplification

*Corresponding author. Email: damien.bigourd@femto-st.fr

to reach very large gain bandwidth, up to 36 THz [14]. In fact, the spectral gain has a temporal distribution since it is induced by the pump instantaneous frequencies. An analytical model has been developed by describing the chirped pulse as an ensemble of independent CW [14] propagating in a fiber owning a constant dispersion profile. Excellent agreements with numerical simulations have been obtained confirming that this analytical tool can be used to interpret the parametric spectrum. When a chirped pulse propagates in a DOF, the instantaneous pump frequency is varied with time while the dispersion profile changes with propagation in the fiber. In this manuscript, we numerically and analytically investigate the generation of MI in this configuration. We also highlight that the side pair is not symmetric in frequency about the pump which is a significant difference from the usual pumping configuration where the fiber is pumped by a CW. The successive instantaneous side band peaks generated by the pump frequencies can even overlap in one side while the spectral locations of instantaneous side bands are relatively well defined in the other side. We believe that this effect can be used to generate tuneable stretched pulse with a wide bandwidth and to amplify ultra-short pulse [15, 16].

2. Methods and description of the investigated cases

2.1. General numerical simulations

In order to deeply investigate the MI when a CW or a chirped pulse is injected in the DOF, realistic numerical simulations have been conducted by integrating the nonlinear Schrödinger equation (NLSE) along the propagation z

$$i \frac{\partial \psi}{\partial z} - \frac{\beta_2(z)}{2} \frac{\partial^2 \psi}{\partial t^2} - i \frac{\beta_{30}}{6} \frac{\partial^3 \psi}{\partial t^3} + \gamma |\psi|^2 \psi = 0 \quad (1)$$

describing the evolution of the slowly varying total electric field ψ in an optical fiber. Eq. 1 has been solved with the standard split-step Fourier including a weak random initial condition that mimics quantum fluctuations. The temporal resolution is 25 fs and the number of points is 2^{16} . Simulated spectra have been averaged over 50 shots and the spectral location of the maximum gain are compared to the analytic derivation presented in the following. The pump pulse has a 10^{th} order super-Gaussian profile with a pulse duration equals to 400 ps at full width half maximum (FWHM). The spectrum is either quasi-monochromatic or broad band. The lossless fiber has a nonlinear coefficient $\gamma=7.5 \text{ W}^{-1} \cdot \text{km}^{-1}$ and the pump power P is 20 W in all cases. For the simulation with the chirped pump pulse, the bandwidth $\Delta\Omega_p$ (FWHM) is changed up to $(1) \times 2\pi$ THz. The chirp is assumed to be linear and is adjusted to keep the same pulse duration, equals to 400 ps. Thus, the chirp is $(2.5) \times 2\pi$ GHz/ps for the maximum bandwidth.

2.2. MI in a fiber with a constant dispersion pumped by a quasi-continuous wave

For comparison to known MI spectrum, we firstly consider a fiber that owns a constant second order dispersion coefficient $\beta_{20}=-0.9 \times 10^{-3} \text{ ps}^2/\text{m}$ and a third order dispersion coefficient $\beta_{30}=+6.8 \times 10^{-5} \text{ ps}^3/\text{m}$. Figure 1.a displays the MI gain profile obtained from the NLSE simulations when the fiber is pumped by a quasi-CW. The fiber length is $L=25$ m. The side lobes are relatively broad and the angular frequency Ω_0 at maximum are located at $\pm 2 \pi \times 2.9$ THz in good agreement with the analytical prediction (vertical dashed lines) given by [2] :

$$\Omega_0 = \pm \sqrt{\frac{-2\gamma P}{\beta_{20}}} \quad (2)$$

The two lobes are symmetric about the pump frequency and their positions can vary with the β_{20} value. However, no MI can be obtained for a positive value within the assumption. Higher order dispersion term should be included [5], for example a negative value of the fourth order of dispersion would allow the appearance of narrow side band.

2.3. MI in a DOF pumped by a quasi-continuous wave

MI has been investigated in several kinds of DOFs [7–12] and we focus this work on a dispersion profile that follows a sinusoidal evolution with the fiber along z with a single period Λ . The total fiber length is $L=50$ m. The second order dispersion at the pump frequency, β_{20} term can be written as :

$$\beta_{20} = \beta_{20av} + \beta_{20amp} \cdot \sin(2\pi z/\Lambda) \quad (3)$$

with β_{20av} the average dispersion and β_{20amp} the amplitude of the variation. When the fiber is pumped by a quasi-CW, it has been shown that non equally spaced sidebands are generated due to a quasi-phase matching condition and the angular frequency shift from the pump Ω_k of the k^{th} band peak can be predicted by [7, 17]:

$$\Omega_k = \pm \sqrt{\frac{\frac{2\pi}{\Lambda}k - 2\gamma P}{\beta_{20av}}} \quad (4)$$

with k an integer.

In the following example, the fiber has a sinusoidal profile (Eq. 3) with an average value $\beta_{20av} = +0.9 \times 10^{-3}$ ps²/m, a modulation amplitude $\beta_{20amp} = +1.6 \times 10^{-3}$ ps²/m and a period $\Lambda = 10$ m. The average third order dispersion coefficient is $\beta_3 = 6.8 \times 10^{-5}$ ps³/m. These parameters are chosen to close matched experimental feasibility and this fiber can be performed in a spectral region around 1 μm [9] or 1.5 μm [18]. In this configuration, the output spectrum exhibits side lobes symmetrically separated about the pump frequency (Figure 1.b). For sake of clarity, we limit the figure to 4 side lobes but the discussion can be done for all k resonant peaks. The frequency of the maximum gain predicted by Eq. 4 is shown with red dashed lines. Good qualitative agreement is obtained although marginal shifts between the simulation and the analytical predictions can be attributed to the approximation in the model [17].

2.4. MI in a DOF pumped by a broad band pulses

When a chirped pump pulse is injected in the same DOF, the dispersion profile varies for each angular pump frequency over the full bandwidth $\Delta\Omega_p$. To analyse the impact of the pump bandwidth, we describe the spectrum as an ensemble of CWs whose angular frequencies are tuned from $-\Delta\Omega_p/2$ to $+\Delta\Omega_p/2$. **The ultra-short pulse is stretched to 400 ps in order to decrease the peak power and thus to generate efficiently the MI with a long pulse without any high-order non linearity.** Therefore, we can assume that each pump angular frequency Ω_p

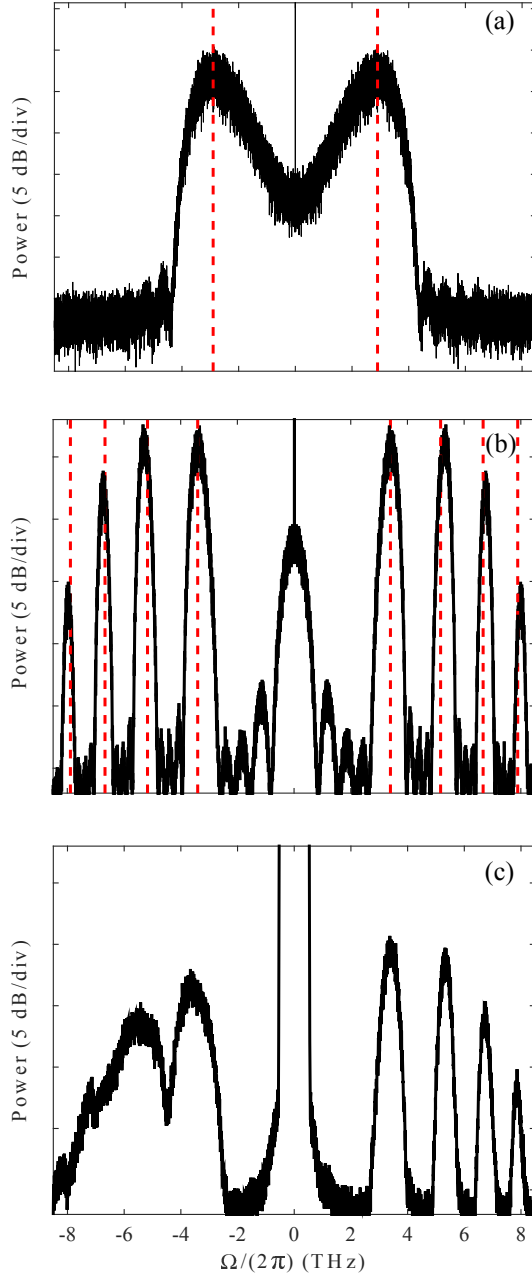


Figure 1. Modulation instability spectrum when (a) a CW pumps a fiber in the anomalous dispersion regime ($\beta_{20} = -0.9 \times 10^{-3}$ ps²/m, $P = 20$ W, $L = 25$ m), (b) a CW pumps the dispersive oscillating fiber ($\beta_{20av} = +0.9 \times 10^{-3}$ ps²/m, $\beta_{20amp} = +1.6 \times 10^{-3}$ ps³/m, $\Lambda = 10$ m, $P = 20$ W, $L = 50$ m), (c) a linear chirped pulse pumps ($T = 400$ ps, $\Delta\omega_p = 2\pi \times 0.8$ THz) the dispersion oscillating fiber.

independently generates the MI since they are temporally separated. This analogy has allowed to obtain excellent results in the case of a fiber with a constant dispersion profile along the fiber [14] and provides an intuitive explanation of the generated spectral components.

In this description, the derivation is achieved with respect to the central pump angular frequency Ω_{p0} as in [14]. Accordingly, the second-order dispersion term depends on $W_p = \Omega_p - \Omega_{p0}$:

$$\beta_2(W_p) = \beta_{20} + \beta_{30} \cdot W_p = \beta_{2av}(W_p) + \beta_{20amp} \cdot \sin(2\pi z/\Lambda) \quad (5)$$

with

$$\beta_{2av}(W_p) = \beta_{20av} + \beta_{30} \cdot W_p \quad (6)$$

assuming that the third order dispersion term is constant along the axial variation and neglecting high order dispersion terms.

From Eq. 4 and Eq. 5, the resonant peaks are obtained for each pump frequency detuning at :

$$\Omega_{k\pm} = \pm \sqrt{\frac{2\pi k - 2\gamma P}{\beta_{2av}(W_p)}} + W_p = \pm |\Omega_{k0}| \cdot \sqrt{\frac{1}{1 + \frac{\beta_{30} \cdot W_p}{\beta_{20av}}}} + W_p \quad (7)$$

with $\Omega_{k0} = \Omega_k(W_p=0)$. The first term takes into account the change of the β_{2av} value when Ω_p is tuned while the second term is used to shift the frame to the central pump frequency ($\Omega_{p0}=0$). For $\frac{\beta_{30} \cdot W_p}{\beta_{20av}} < 1$, this expression can be expanded up to the second order as

$$\Omega_{k\pm} \approx \pm |\Omega_{k0}| + W_p \left(1 \mp \frac{1}{2} B |\Omega_{k0}| \pm \frac{3}{8} B^2 W_p |\Omega_{k0}|\right) \quad (8)$$

with $B = \frac{\beta_{30}}{\beta_{20av}}$. When Ω_p is tuned away from the central angular frequency Ω_{p0} ($W_p \neq 0$), the resonant peaks are shifted by the second term in Eq. 8. In this frequency frame, the side bands are not shifted by the same amounts in the Stokes and anti-Stokes sides and it depends on $B \cdot W_p$ and Ω_{k0} . Accordingly, we label the k^{th} peak as $k+$ and $k-$ for the positive and negative frequency shifts, respectively.

Figure 1.c shows an example of a MI spectrum simulated with NLSE when the 400 ps pulse injected in the DOF has a bandwidth equals to $(0.8) \times 2\pi$ THz. The spectrum is not symmetric about the pump and is broad in the Stokes side while the anti-Stokes sides seems similar to the case when the CW pumps the DOF (Figure 1.b). In the following, we aim to explain and discuss this observation with the previous analytical derivations and the simulations.

To numerically interpretate the spectrum, we performed simulations with spectrally shifted CWs. All the output spectra are shifted to the center of the pump bandwidth, Ω_{p0} ($W_p=0$ THz) and compared to the bands generated with the chirped pulse. We assume that all instantaneous MI are independently generated from each other. In our analysis, the chirp pulse is sampled by N spectrally shifted CWs over the bandwidth with the same spectral profile as the chirped pulse. As the pulse is linearly chirped, the spectrum has also a super-Gaussian profile with a bandwidth $\Delta\Omega_p$ (FWHM). All the MI bands has been centered to Ω_{p0} and the output integrated spectrum $S(\Omega)$ is obtained by taking the square of the sum of all the electric field $\tilde{\psi}$ in the frequency domain :

$$S(\Omega) \propto \left| \sum_{W_p = -\Delta\Omega_p/2}^{+\Delta\Omega_p/2} \tilde{\psi}(\Omega - W_p, W_p) \right|^2 \quad (9)$$

3. Impact of the pump bandwidth on the modulation instability

3.1. Spectral evolution with the pump frequency and bandwidth

In order to discuss the asymmetry of the MI spectrum, we investigated the evolution of the MI with the pump frequency. Figure 2 shows the angular frequency shift of the lobes in the Stokes (Ω_{k-}) and Anti-Stokes (Ω_{k+}) sides as a function of W_p tuned from $(-0.8)\times 2\pi$ to $(+0.8)\times 2\pi$ THz obtained with Eq. 7 (solid line) and its expansion (Eq. 8-dash line). The two curves are in good agreement for this pump scan. For the three first side lobes, the frequency variation of Ω_{k-} is more important than the one of Ω_{k+} . For example, Ω_{2-} varies by nearly $(4)\times 2\pi$ THz while Ω_{2+} changes only by $\sim (0.5)\times 2\pi$ THz. With opposite value of β_3 , we checked that the spectral extension is more important in the Anti-Stokes side (not shown), as expected from the analytical expression (Eq. 8). With this large spectral shift, two subsequent resonant peaks can be generated at the same angular frequency but from different pump frequency, i.e $\Omega_k(W_{p1})=\Omega_{k+1}(W_{p2})$. To illustrate this comment, $\Omega_k(W_p=0)$ and $\Omega_{k+1}(W_p=0)$ are also plotted in Figure 2. In this case, Ω_{2-} and Ω_{3-} expands up to $\Omega_3(W_p=0)$ and $\Omega_4(W_p=0)$ at $W_p\sim(-0.59)\times 2\pi$ THz and $W_p\sim(-0.4)\times 2\pi$ THz, respectively. This means that several bands generated by a chirped pulse cannot be distinguished in the spectral domain since they overlap.

Figure 3.a displays the simulated spectrum when the frequency of the CW pump is tuned and selected spectral profiles are shown for W_p equals to $(-0.4)\times 2\pi$, $(0)\times 2\pi$ or $(+0.4)\times 2\pi$ THz (Figure 3.b). The bands in the Stokes side clearly shift away from the pump while the band centers in the Anti-Stokes side are relatively unchanged when the pump is tuned. We remind the reader that the spectra are shifted to the center of the pump frequency scan. In the usual representation, the bands are symmetric about the pump frequency. The green lines are given by Eq. 7 and are in good agreement with the maximum obtained by the simulation. The quantitative disagreements between the simulations and the analytical predictions have also been observed in Figure 1.b. As already observed in Figure 2, subsequent bands can be generated at the same angular frequency but from different pump frequencies. In addition, the maximum gain varies with the pump frequency. For example, the gain changes by only 6 dB and 2 dB for $k=1$ and 2, when the pump frequency is changed from -0.4 to 0.4 THz (Figure 3.b). The change is more important for $k=3$, it changes by ~ 12 dB.

When the chirped pulse is injected in the same fiber, the spectral width of each band in the Anti-stokes side is narrow (~ 0.35 THz at FWHM) as in the previous case with the CW excitation and is relatively constant when the pump bandwidth ($\Delta\Omega_p$) is tuned (Figure 3.d). Alternatively, the bands broaden in the Stokes side and for large pump bandwidth, successive side bands tend to overlap leading to a large spectrum (Figure 3.c). The $k=3$ and 4 bands shift to lower frequency shift when the pump bandwidth increases (Figure 3.c). This is due to the change of the maximum gain with pump frequency as observed in the CW mode. For example, for $\Delta\Omega_p=(+0.8)\times 2\pi$ THz (black line), all the frequency components lying in the pulse are between $(\pm 0.4)\times 2\pi$ THz in Figure 3.a. Therefore, the bands overlap and cannot be distinguished. The separation between the two first lobes at ~ -4.5 THz still exists even for $\Delta\Omega_p=(0.8)\times 2\pi$ at FWHM (Figure 3.b black line and Figure 3.d) because the band at $k=1$ shifts less with the pump frequency than the other bands (Figure 3.a). In addition, the MI generated at the edge of the pump bandwidth (at $\pm 0.4\times 2\pi$ THz) is generated with a power twice smaller (i.e 10 W) leading to a drop of the gain by more than 10 dB. The shape of the bands excited by a chirped pulse can also be more precisely inferred from the band obtained with CWs. For the Super-Gaussian pump profile with $\Delta\Omega_p=(0.8)\times 2\pi$, the pulse has been sampled in $N=60$ spectrally shifted CWs over the bandwidth with the same spectral profile as the chirped pulse. All the MI bands has been centered to Ω_{p0} and the output spectrum is obtained from Eq. 9. This analogy with independent CW waves (Figure 3 d-grey curve) is in excellent agreement with the MI bands obtained directly with the chirped pulse confirming the correct interpretation of the generated MI.

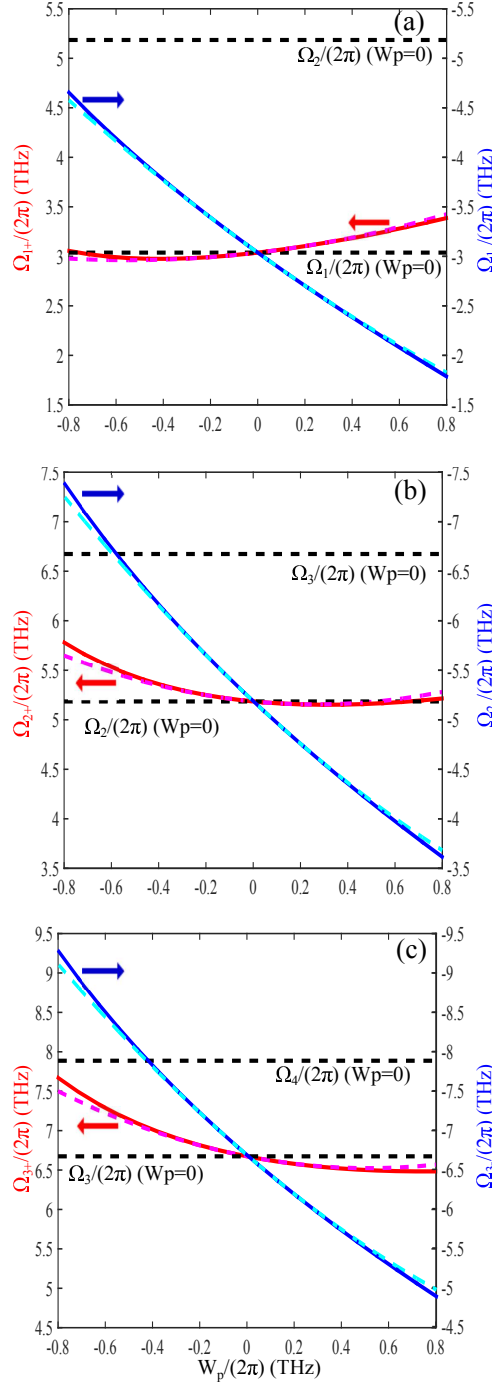


Figure 2. Evolution of $\Omega_{k+}/(2\pi)$ (red line) and $\Omega_{k-}/(2\pi)$ (blue line) as a function of the pump frequency detuning for $k=1$ (a), $k=2$ (b) and $k=3$ (c). Solid lines are calculated from Eq. 7 and the dashed lines correspond to the expansion (Eq.8). $\Omega_k/(2\pi)$ and $\Omega_{k+1}/(2\pi)$ at $W_p = 0$ THz are also displayed.

3.2. Temporal distribution and parametric amplification

In addition to the asymmetry in the MI spectrum, the difference in the Stokes and anti-Stokes sides also occurs in the temporal domain. Indeed, the MI spectrum generated by the broadband pulse has a spectro-temporal distribution since it is generated by a chirped pulse. The instantaneous angular frequency shift can be written in the time domain; $\alpha \cdot \tau$. An

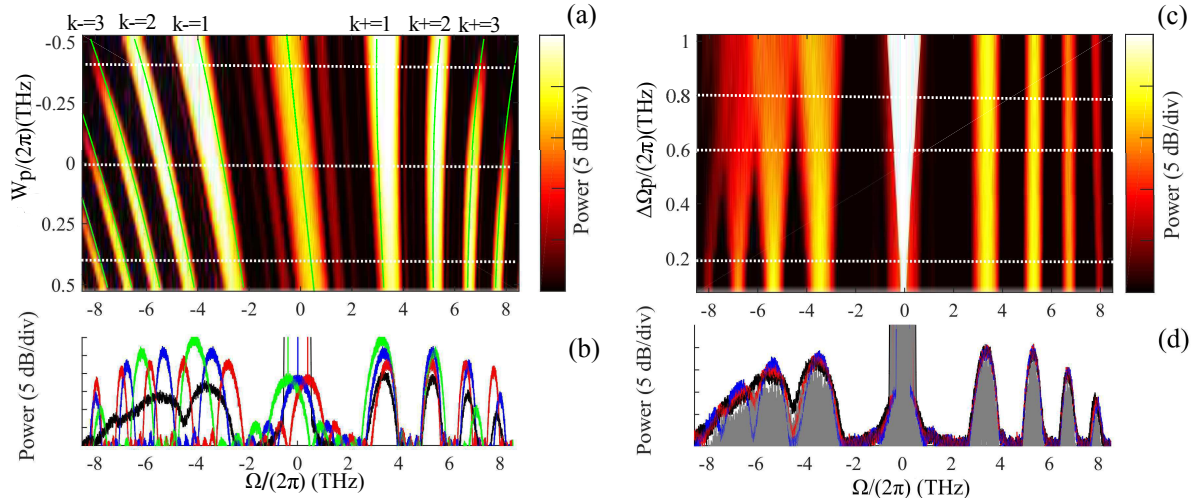


Figure 3. (a) Evolution of the MI spectrum simulated with the NLSE as a function of the pump frequency shift of CWs ($P=20$ W). Green lines are the frequency at maximum gain for each k band predicted by Eq. 5 (b) Selected profiles for $\Delta\Omega_p/(2\pi)=-0.4$ THz (green line), 0 THz (blue line) and 0.4 THz (red line). (c) Evolution of the MI spectrum as a function of the pump bandwidth for a chirped pulse. (d) Selected profiles for $\Delta\Omega_p/(2\pi)=0.4$ THz (blue line), 0.6 THz (red line) and 0.8 THz (black line). Spectrum of the sum of CW waves over 0.8 THz (grey curve) with the same spectral profile as the chirped pulse.

interferogram is shown in Figure 4 for a bandwidth equals to $(0.8)\times 2\pi$ THz (FWHM). Dash green lines are obtained from Eq. 7. As expected from Section 3.1, the bandwidth in the Anti-Stokes side is narrow and relatively unchanged over the full temporal profile, i.e. ~ 400 ps. In the Stokes side, the induced chirp is higher leading to a larger bandwidth. For example, for $k=-1$ the chirp is $\sim (3.4)\times 2\pi$ GHz/ps while it is $\sim (0.6)\times 2\pi$ GHz/ps for $k+=1$. If β_3 has an opposite sign, the chirp is higher in the Anti-Stokes side (not shown) as expected from Eq. 8.

The spectro-temporal distribution has a direct impact on the parametric amplification when a CW is injected at maximum gain of the band since the spectral gain is temporally shifted. Figure 5 shows the spectrum in the unsaturated regime when a CW signal is injected at the maximum of each side lobes at $\Omega=\pm 3.4, 5.3$ or 6.7 THz. During propagation, the CW signal is instantaneously amplified when the gain exists and an idler pulse is generated. From photon energy conservation in a four wave mixing process, the maximum bandwidth of the signal can be twice the pump bandwidth (2×0.8 THz) if all the waves are phase matched [19]. However, the CW signal interacts with the instantaneous spectral gain in a temporal window shorter than the full pump pulse. The CW interacts during a longer temporal width when it is injected in the Stokes side rather than in the anti-Stokes side. Accordingly, the bandwidth (FWHM) is broader for $k=-1-3$ (0.89 THz, 1.18 THz, 0.75 THz) while it is much narrower (0.54 THz, 0.33 THz, 0.21 THz) when the CW signal is injected in the Stokes side.

4. Conclusion

We have numerically investigated the spectral properties of MI generated in a DOF pumped by a broad band pulse. We addressed that the spectrum can be large and is not symmetric as respect to the pump spectrum. The spectral distribution can be intuitively understood with an analogy with MI generated with CW waves. Each instantaneous frequency generates their own spectrally shifted MI with a different chirp in the Stokes or Anti-Stokes sides leading to a spectral broadening in only one band. This method is promising to generate tuneable stretched pulses with a wide bandwidth by selecting the idler when a CW signal is injected in the fiber.

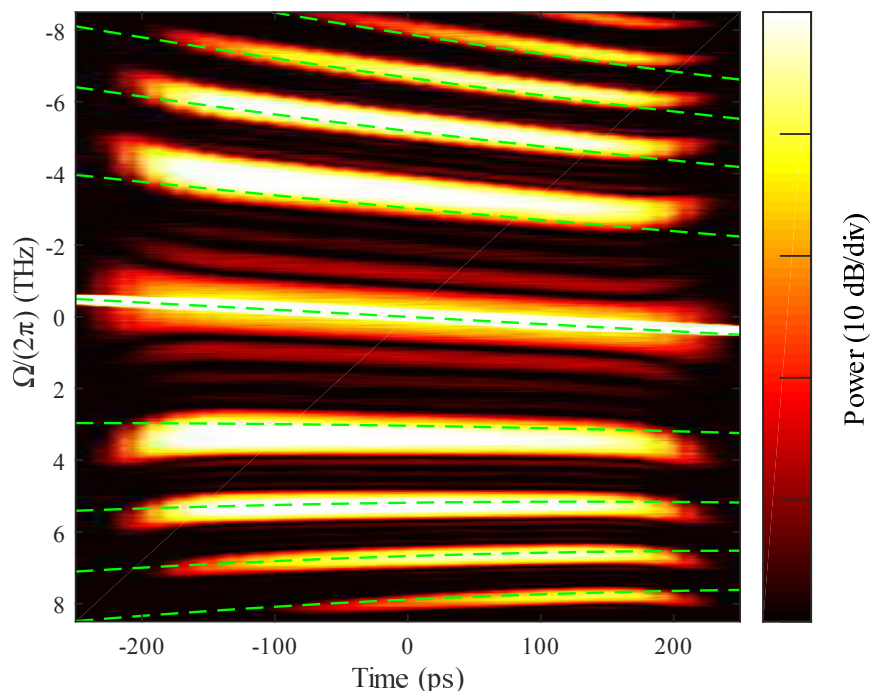


Figure 4. Logarithmic scale spectrogram of the electric field at the output fiber when the chirped pulse is injected with $\Delta\Omega_p=(0.8)\times 2\pi$ THz.

Acknowledgments. Computations have been performed on the supercomputer facilities of the Mésocentre de calcul de Franche Comté.

References

- [1] K. Tai, A. Hasegawa, A. Tomita, "Observation of Modulational Instability in Optical Fibers," *Phys. Rev. Lett.* **56**, 135 (1986)
- [2] G. P. Agrawal, *Nonlinear Fiber Optics* (Academic, 2013)
- [3] Z. Lali-Dastjerdi, K. Rottwitt, M. Galili, C. Peucheret, "Asymmetric gain saturated spectrum in fiber optical parametric amplifiers," *Opt. Express*, **20**, 15530 (2012)
- [4] A. Mussot, A. Kudlinski, R. Habert, I. Dahman, G. Mlin, L. Galkovsky, A. Fleureau, S. Lempereur, L. Lago, D. Bigourd, T. Sylvestre, M. W. Lee, and E. Hugonnot, "20 THz-bandwidth continuous-wave fiber optical parametric amplifier operating at 1 μm using a dispersion-stabilized photonic crystal fiber," *Opt. Express*, **20**, 28906 (2012)
- [5] S. Pitois, G. Millot, "Experimental observation of a new modulation instability spectral window induced by fourth order dispersion in a normally dispersive single-mode optical fiber," *Opt. Comm.* **226**, 415 (2003)
- [6] J. Rothenberg, "Modulational instability for normal dispersion," *Phys. Rev. A* **42**, 682 (1990)
- [7] N.J Smith, N. J. Doran, "Modulational instabilities in fibers with periodic dispersion management," *Opt. Lett.* **21** 570 (1996)
- [8] F.K. Abdullaev, S.A . Damanyan, A. Kobayakov, F. Lederer, "Modulation instability in optical fibers with variable dispersion," *Phys. Lett. A*, **220**, 213 (1996)
- [9] M. Droques, A. Kudlinski, G. Bouwmans, G. Martinelli, A. Mussot, "Experimental demonstration of modulation instability in an optical fiber with a periodic dispersion landscape," *Opt. Lett.* **37**, 4832 (2012)
- [10] F. Feng, P. Morin, Y. K. Chembo, A. Sysoliatin, S. Wabnitz, C. Finot, "Experimental demonstration

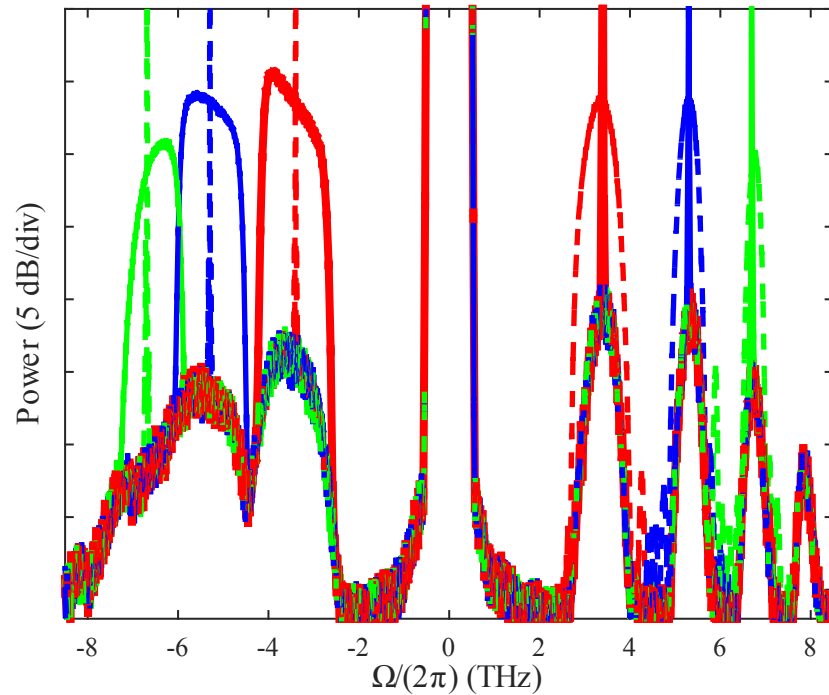


Figure 5. Output spectra when a CW signal is injected at the maximum of each side lobes ± 3.4 , 5.3 or 6.7 THz together with a stretched pulse ($\Delta\Omega_p=(0.8)\times 2\pi$ THz).

- of spectral sideband splitting in strongly dispersion oscillating fibers," *Opt. Lett.* **40**, 455 (2015)
- [11] C. Fourcade-Dutin, A. Bassery, D. Bigourd, A. Bendahmane, A. Kudlinski, M. Douay, A. Mussot, "12 THz flat gain fiber optical parametric amplifiers with dispersion varying fibers," *Opt. Express* **23** 10103 (2015)
- [12] C. Finot, A. Sysoliatin, S. Wabnitz, "Nonlinear parametric resonances in quasiperiodic dispersion oscillating fibers," *Opt. Comm.* **348**, 24 (2015)
- [13] D. Bigourd, P. Beaurès, J. Dubertrand, E. Hugonnot, A. Mussot, "Ultra-broadband fiber optical parametric amplifier pumped by chirped pulses," *Opt. Lett.* **13**, 3782 (2014)
- [14] O. Vanvincq, C. Fourcade-Dutin, A. Mussot, E. Hugonnot, D. Bigourd, "Ultra-broad band fiber optical parametric amplifier pumped by chirped pulses Part I : Analytical model," *J. Opt. Soc. Am. B* **32** 1479 (2015)
- [15] C. Fourcade-Dutin, O. Vanvincq, A. Mussot, E. Hugonnot, D. Bigourd, "Ultra-broad band fiber optical parametric amplifier pumped by chirped pulses Part II : Sub-30 fs pulse amplification at high gain," *J. Opt. Soc. Am. B* **32** 1488 (2015)
- [16] D. Bigourd, L. Lago, A. Mussot, A. Kudlinski, J. F Gleyze, E. Hugonnot, "High-gain fiber, optical parametric chirped pulse amplification of femtosecond pulses at $1 \mu\text{m}$," *Opt. Lett.* **35**, 3480 (2010)
- [17] M. Droques, A. Kudlinski, G. Bouwmans, G. Martinelli, A. Mussot, "Dynamics of the modulation instability spectrum in optical fibers with oscillating dispersion," *Phys. Rev. A* **87**, 013813 (2013)
- [18] X. Wang, D. Bigourd, A. Kudlinski, K. K. Y. Wong, M. Douay, L. Bigot, A. Lerouge, Y. Quiquempois, A. Mussot, "Correlation between multiple modulation instability side lobes in dispersion oscillating fiber," *Opt. Lett.* **39**, 1881 (2014)
- [19] B.P.P. Kuo, S. Radic, "Fast wideband source tuning by extra-cavity parametric process," *Opt. Express* **18**, 19930 (2010)